RADIATION RESEARCH **202**, 706–718 (2024)
0033-7587/24 $15.00

DOI: 10.1667/RADE-24-00126.1

Mitigating the Effects of 1-Palmitoyl-2-linoleoyl-3-acetyl-rac-glycerol on Gastrointestinal Acute Radiation Syndrome after Total-Body Irradiation in Mice

Jinseon Jeong,[a,1] Sojung Sun,[a,b,1] Yong-Jae Kim,[a] Ki-Young Sohn,[a] Jae Wha Kim,[c,2] Jae Sam Lee[a,2]

[a] R&D institute, Enzychem Lifesciences, Suwon 16229, Republic of Korea; [b] Department of Radiation Oncology, Korea Institute of Radiological and Medical Sciences, Seoul 01812, Republic of Korea; [c] Division of Biomaterials Research, Korea Research Institute of Bioscience and Biotechnology, Daejeon 34141, Republic of Korea

Jeong J, Sun S, Kim Y-J, Sohn K-Y, Kim JW, Lee JS. Mitigating the Effects of 1-Palmitoyl-2-linoleoyl-3-acetyl-rac-glycerol on Gastrointestinal Acute Radiation Syndrome after Total-Body Irradiation in Mice. Radiat Res. 202, 706–718 (2024).

Total-body irradiation (TBI) with gamma rays can damage organisms in various unexpected ways and trigger several organ dysfunction syndromes, such as acute radiation syndrome (ARS). Hematopoietic cells and enterocytes are particularly sensitive to radiation due to their self-renewal ability and rapid division, which leads to hematopoietic ARS (H-ARS) and gastrointestinal ARS (GI-ARS). We previously showed that a lipid-based small molecule, 1-palmitoyl-2-linoleoyl-3-acetyl-rac-glycerol (PLAG), improved 30-day survival and alleviated H-ARS symptoms in BALB/c mice after a lethal dose ($LD_{70/30}$) of gamma-ray TBI. In this study, we investigated the mitigating effects of PLAG on radiation-induced GI damage that occurs under the same conditions as H-ARS in BALB/c mice. Our study showed that PLAG facilitated the structural restoration of intestinal tissues by increasing villus height, crypt depth, crypt number, mucin-producing goblet cells, and proliferating cell nuclear antigen (PCNA)-positive crypt cells. PLAG significantly improved intestinal absorptive capacity and reduced intestinal injury-induced bacterial translocation. In addition, PLAG effectively inhibited radiation-induced necroptosis signaling activation in the intestinal crypt cells, which was responsible for sustained tissue damage and the release of high mobility group box 1 (HMGB1), a typical damage-associated molecular pattern. Overall, our findings support the radiation-mitigating potential of PLAG against GI-ARS after accidental radiation exposure.

INTRODUCTION

Exposure to high doses of ionizing radiation (radiation) can cause multiple organ dysfunction syndromes, collectively known as acute radiation syndrome (ARS) (*1*). ARS is largely categorized into three distinct sub-syndromes differentiated by clinical and physiological symptoms (not molecular pathophysiological processes): hematopoietic ARS (H-ARS), gastrointestinal ARS (GI-ARS), and neurovascular ARS (NV-ARS) (*2–4*). A growing body of literature indicates that GI damage is a key cause of radiation-induced mortality and morbidity in mammals, including humans (*5*) because tissues with rapid cellular turnover in the gastrointestinal system are more susceptible to the detrimental effects of ionizing radiation (*6*). In particular, radiation damage to the intestinal stem cells residing within the crypt base can impair their self-renewal potential, leading to shortening of the crypts and villi, loss of mucosal barrier, and septic shock (*7*). Despite the increasing threat of unexpected and accidental radiation exposure, there are currently no radiation countermeasures against GI-ARS approved by the US Food and Drug Administration (FDA)(*8*). Therefore, radioprotective or radiomitigating agents that alleviate GI-ARS symptoms should be developed urgently.

The high sensitivity of the GI system to radiation is attributed to the extremely rapid cell turnover rate of the intestinal epithelium. Arike et al. estimated epithelial cell turnover to be 3–5 days in the small intestine and 5–7 days in the colon (*9*). Therefore, GI-ARS symptoms such as anorexia, severe nausea, vomiting, abdominal cramping, and diarrhea, manifest within hours to days of exposure (*10*). If proper medical care is not provided, victims will die within days or weeks of radiation exposure owing to dehydration, loss of electrolytes, malabsorption, infectious complications caused by bacterial translocation through the impaired mucosal barrier, and septic shock (*11*). As we have mentioned above, there are currently no FDA-approved drugs to protect or to mitigate GI-ARS, and four FDA-approved drugs, namely, Neupogen®, Neulasta®, Leukine®, and Nplate®, to treat H-ARS are known to have minimal effects on GI-ARS (*12*, *13*). Currently, it is best to follow the basic guidelines for the medical management of patients with GI-ARS, including the use of supportive care, refinement based on NHP medical countermeasure studies, and/or stem cell growth factor supplementation (*14*).

The devastating effect of radiation on rapidly proliferating cells, like active intestinal stem cells and progenitor

[1] These authors contributed equally to this work.

[2] Corresponding authors: Jae Wha Kim, PhD, Cell Factory Research Center, Division of Systems Biology and Bioengineering, Korea Research Institute of Bioscience and Biotechnology, Korea Research Institute of Bioscience and Biotechnology, 125 Gwahak-ro, Yuseong-gu, Daejeon 305-333, Republic of Korea; email: wjkim@kribb.re.kr. Jae Sam Lee, PhD, R&D Institute, Enzychem Lifesciences, Suwon 16229, Republic of Korea; email: jaesam.lee@enzychem.com; jsfemto@gmail.com.

cells, residing within the proliferative compartment of the crypts of Lieberkühn (*15*). These cell types undergo apoptosis induced by DNA damage and free radicals produced by water hydrolysis within the initial 1–2 days after radiation exposure (*16*). In addition to direct cell death by radiation, surviving cells continue to be threatened by death caused by pro-inflammatory cytokines, damage-associated molecular patterns (DAMPs), and bacteria invading the intestinal lumen (*17*). Necroptosis, also called regulated necrosis, is an immunogenic form of cell death that requires the activation of receptor-interacting protein kinase-1 (RIPK1), RIPK3, and mixed lineage kinase domain-like (MLKL) (*18*). Activated RIPK1 forms a complex with RIPK3 that subsequently phosphorylates MLKL to form MLKL oligomers. MLKL oligomers are translocated from the cytosol to the plasma membrane, forming pores that increase membrane permeabilization and eventually cause cell disruption (*18*). Necrostatin-1, a RIPK1 inhibitor, attenuates RIPK3 serine phosphorylation in the ileum and improves survival 48 h after total-body irradiation (TBI) in C57BL/6NTac mice, implying that necroptosis contributes to radiation-induced cell death (*19*).

1-Palmitoyl-2-linoleoyl-3-acetyl-rac-glycerol (PLAG) is a synthetic triacylglycerol containing two long-chain fatty acid groups (palmitic and linoleic acids) at the 1st and 2nd position, as well as an acetyl group at the 3rd position of the glycerol backbone. PLAG was granted Orphan Drug Designation for the treatment of ARS by the FDA in 2018. In our previous studies, we demonstrated the potential of PLAG as a radiation countermeasure against H-ARS in 11-week-old BALB/c mice by exposing them to a lethal dose ($LD_{70/30}$, 6.11 Gy) of gamma-ray TBI (*20*, *21*). In this study, we found that several symptoms of GI-ARS manifested under the same experimental conditions as those of H-ARS in TBI mice. This finding led us to investigate whether PLAG mitigates radiation-induced GI damage in TBI mice 24 h after irradiation. Our results show that PLAG rapidly regenerates the intestinal epithelium and restores the normal functions of the GI tract, such as nutrient absorption and protection of the intestinal mucosal barrier. Moreover, PLAG effectively prevented TBI-induced sustained tissue damage by regulating the necroptosis signaling pathway and the release of high mobility group box *1* (HMGB1), a typical endogenous damage-associated molecular pattern (DAMP).

MATERIALS AND METHODS

Animals and Ethics Statement

Specific pathogen-free (SPF) male BALB/c mice (10 weeks old) were purchased from Koatech Co. (Pyeongtaek, Korea). The mice were housed in an SPF facility under consistent temperature and light/dark cycles. Animals were fed a standard diet and water ad libitum. Animal experiments were performed after one week of acclimatization, and five mice per cage were assigned according to their body weight. All experimental procedures were performed in accordance with the Institutional Animal Care and Use Committee (IACUC) of the Korea Research Institute of Bioscience and Biotechnology and were performed in compliance with the "Guide for the Care and Use of Laboratory Animals" by the National Research Council and Korean national laws for animal welfare.

Animal Experiment

Irradiation and PLAG administration were performed as previously described (*22*). Briefly, male_BALB/c mice (11 weeks old) were placed in single chambers of a lead-shielded irradiation apparatus and exposed to a single, uniform dose of total-body γ-ray irradiation from a ^{60}Co source (J.L. Shepherd & Associates, San Fernando, CA) at a dose rate of 0.833 Gy/min. Dose rates were measured using an EPD Mk2+ electronic dosimeter (Thermo Scientific™, Waltham, MA). PLAG was synthesized by Enzychem Life Sciences Corp. (Jecheon, Korea) and resuspended in sterile phosphate-buffered saline (PBS). Mice received 250 mg/kg of PLAG [0.1 ml/mouse, oral (p.o.) administration] or vehicle [sterile PBS; 0.1 mL/mouse, (p.o.) administration] beginning 24 h postirradiation and continued daily until 21 days postirradiation.

Histological Analysis

Mice were euthanized, and small intestine tissues (jejunum) were isolated on days 0, 1, 3, 7, 15, and 21 after TBI. Tissues were fixed with 10% formalin overnight and transferred to the Korea Pathology Technical Center (Cheongju, South Korea) for paraffin embedding and hematoxylin and eosin (H&E) staining. Images of the small intestine sections were captured using a Leica Flexacam C3 microscope (Wetzlar, Germany). Intestinal sections were used to measure villus height, crypt depth, and the number of crypts per field of view (FOV). For the measurement of villus height and crypt depth, the numbers of villi and crypts assessed per mouse were 35 and 45, respectively. For the determination of crypt numbers, 5 FOV per section were assessed.

The degree of goblet cell population was assessed in jejunal sections from mice at days 1, 3, 7, 15, and 21 after TBI using an Alcian Blue staining kit (Vector, Newark, CA) according to the manufacturer's instructions. After completing the assay, the slides were examined by light microscopy using a Leica Flexacam C3 microscope (Wetzlar, Germany).

Immunohistochemical Analysis

For immunohistochemical analysis, the de-paraffinized and hydrated sections were heated in antigen retrieval buffer for 10 min and stained with rabbit monoclonal PCNA (Cell Signaling Technology, Danvers, MA), HMGB1 (Abcam, Cambridge, UK) and phospho-MLKL (Invitrogen, Carlsbad, CA) antibodies at 4°C overnight after blocking with 10% fetal bovine serum in PBS. Visualization was performed using a DAKO Real Envision detection system according to the manufacturer's instructions, and the sections were counterstained with hematoxylin. Images of the small intestine sections were captured using a Leica Flexacam C3 microscope (Wetzlar, Germany). For quantification, 4–5 fields of view per section were assessed using ImageJ software (National Institutes of Health, MD) by calculating the 3,3′-diaminobenzidine positive area using a color threshold.

D-xylose Absorption Assay

A D-xylose absorption assay was performed to examine the regenerative capacity of the intestine as a physiological indicator of mucosal barrier integrity, as described by Venkateswaran et al. (*11*). Briefly, the mice were fasted for 4 h and then orally administered 200 mg/kg D-xylose dissolved in saline. The minimal amount of blood (100–200 μL) was collected 2 h after D-xylose administration from the orbital sinuses using EDTA-free capillary tubes (Kimble Chase Life Science and Research Products LLC, Vineland, NJ) and 1.5 mL microcentrifuge tubes. The blood-containing tubes were centrifuged at 6,000 rpm for 20 mins at 4°C to separate serum. A total of 50 μL of serum samples was mixed with 5 mL of phloroglucinol reagent (0.5 g of phloroglucinol, 100 mL of glacial acetic acid, and 10 mL of concentrated HCl) and heated in a water bath at 100°C for

5 min. After cooling down, the absorbance of the samples was measured at a wavelength of 554 nm using a spectrophotometer.

Enterococcus Feacalis Oral Infection-Induced Bacterial Translocation in TBI Mice

The effect of PLAG on infectious complications caused by intestinal injury-induced spontaneous bacterial translocation in TBI mice was investigated using (i) mortality rates, (ii) occurrence rates of positive bacterial cultures, and (iii) bacterial growth in the blood, lungs, and liver tissues of TBI mice. *Enterococcus faecalis,* a commensal bacterium inhabiting the human gastrointestinal tract, was obtained from the Korean Collection for Type Cultures (Jeong-eup, South Korea) and used as an infectious agent in this study because oral infection with *E. faecalis*-induced bacterial translocation and septic death in TBI mice after antibiotic decontamination as per previous studies (*23*, *24*). The mice were decontaminated by providing water containing an antibiotic cocktail (AC, 4 mg/ml penicillin, streptomycin, and bacitracin) for 7 days before and 6 days after TBI. To stabilize *E. faecalis* oral infection, the mice were orally treated with lansoprazole (a proton pump inhibitor, 0.5 mg/0.1 mL/mouse) on day 5 after TBI. The day after lansoprazole treatment, the mice were then orally infected with 3×10^5 CFU of *E. faecalis* per mouse, and AC was removed from the drinking water. The mice were monitored at least twice daily for 15 days for *E. faecalis* oral infection. On days 1, 3, 5, and 7 after *E. faecalis* oral infection, blood was collected from the orbital sinuses, and the lungs and liver were excised and homogenized. Blood and homogenized tissue samples were diluted with sterile PBS, spread on tryptic soy agar plates, incubated at 37°C for 18 h, and the number of colonies was counted.

Western Blot

The levels of circulating HMGB1 in the mouse serum were examined as previously described (*25*). Briefly, 3 μL of the serum was diluted with 72 μL of 1 × SDS sample buffer and heated at 95°C for 5 min. Samples were separated on a 12% polyacrylamide gel using SDS sulfate-polyacrylamide gel electrophoresis. The gel was then transferred onto a polyvinylidene difluoride (PVDF) membrane. Rabbit monoclonal HMGB-1 antibody (Abcam) was used as the primary antibody. The blots were then incubated with a secondary antibody and visualized using the SuperSignal™ West Femto Maximum Sensitivity Substrate (Thermo Scientific™). Protein membranes were stained with Ponceau S solution (Sigma-Aldrich, Burlington, MA) for total protein normalization. The density of the Western blot bands was calculated using ImageJ software to quantify protein expression levels.

Statistical Analyses

All error bars indicate the standard deviation (SD), and all data were analyzed using unpaired Student's t-test or one-way analysis of variance (ANOVA), followed by the Tukey-Kramer post hoc test. Statistical significance was set at $P < 0.05$. Statistical analyses were performed using GraphPad Prism version 8.4.3 (GraphPad, La Jolla, CA).

RESULTS

PLAG Mitigates Gastrointestinal Damage in Irradiated Mice

To assess the extent of gastrointestinal damage caused by TBI, hemorrhage, and structural injury to the GI tract were macroscopically observed after laparotomy. On day 15 after TBI, a laparotomy was performed to observe the GI tract because previous studies showed that irradiated mice suffered severe weight loss and started to die around 15 days after TBI (*20*, *21*). As shown in Fig. 1A, the mass of visceral adipose tissue in the 6.11 Gy TBI-only group was considerably lower than that in the non-irradiated group. The PLAG-treated group exhibited substantial recovery of the visceral adipose mass. Moreover, multiple hemorrhagic spots were observed in all three parts of the small intestine in the 6.11 Gy TBI-only group compared with the non-irradiated group. Administration of PLAG substantially decreased radiation-induced gastrointestinal hemorrhage (Fig. 1B).

PLAG Facilitates the Structural Restoration of the Intestinal Tissues Damaged by TBI

Next, we assessed whether PLAG mitigated radiation-induced GI tract damage by examining histological changes within the jejunal part of the small intestine. As shown in Fig. 2A, crypt atrophy and villus blunting were observed on the interior surface of the jejunum as early as days 1 and 3 after TBI in both groups. The destruction of the intestinal epithelium worsened at days 7 and 15 after TBI in the 6.11 Gy TBI-only group. The damaged intestinal epithelium was not completely restored to normal status until day 21 in the 6.11 Gy TBI-only group. In contrast, the crypt-villi structures of the small intestines were restored in the 6.11 Gy TBI + PLAG group at days 7, 15, and 21 after TBI (Fig. 2A). In addition, we investigated the effects of TBI and PLAG on intestinal injury parameters by measuring villus height, crypt depth, and the number of crypts per field in small intestinal tissues (Fig. 2B–D). A significant reduction in villus height was observed on days 1, 3, 7, and 15 after TBI compared to day 0 (no irradiation), whereas daily administration of PLAG significantly increased villus height from day 3 after TBI (Fig. 2B). Radiation-induced alterations in crypt morphology were quantified by measuring crypt depth and the number of crypts per field. The crypt depth dramatically decreased from day 1 after TBI and remained significantly lower than day 0 (non-irradiated) until day 15 after TBI, whereas PLAG significantly increased the crypt depth from day 3 after TBI (Fig. 2C). In addition, a sharp decline in crypt numbers per field was observed from day 1 to day 15 after TBI in the 6.11 Gy TBI group compared with day 0 (no irradiation) and the PLAG-treated group. Collectively, these findings indicate that PLAG effectively ameliorates radiation injury by facilitating the recovery of the epithelial architecture of the small intestine.

PLAG Increases Mucin Secretion by Promoting the Recovery of Goblet Cells in The Intestinal Tissues Damaged after TBI

The intestinal mucosal layer is the first line of defense against intestinal microorganisms, digestive enzymes, acids, microbes, and food-associated toxins. Goblet cells are a type of intestinal epithelial cells whose primary function is to synthesize and secrete mucus (*26*). Next, we investigated whether PLAG mitigates the destruction of goblet cells in the damaged GI tract after TBI by staining the jejunal sections with Alcian blue. Alcian blue staining (Fig. 3A) and corresponding densitometry (Fig. 3B) showed that the number of

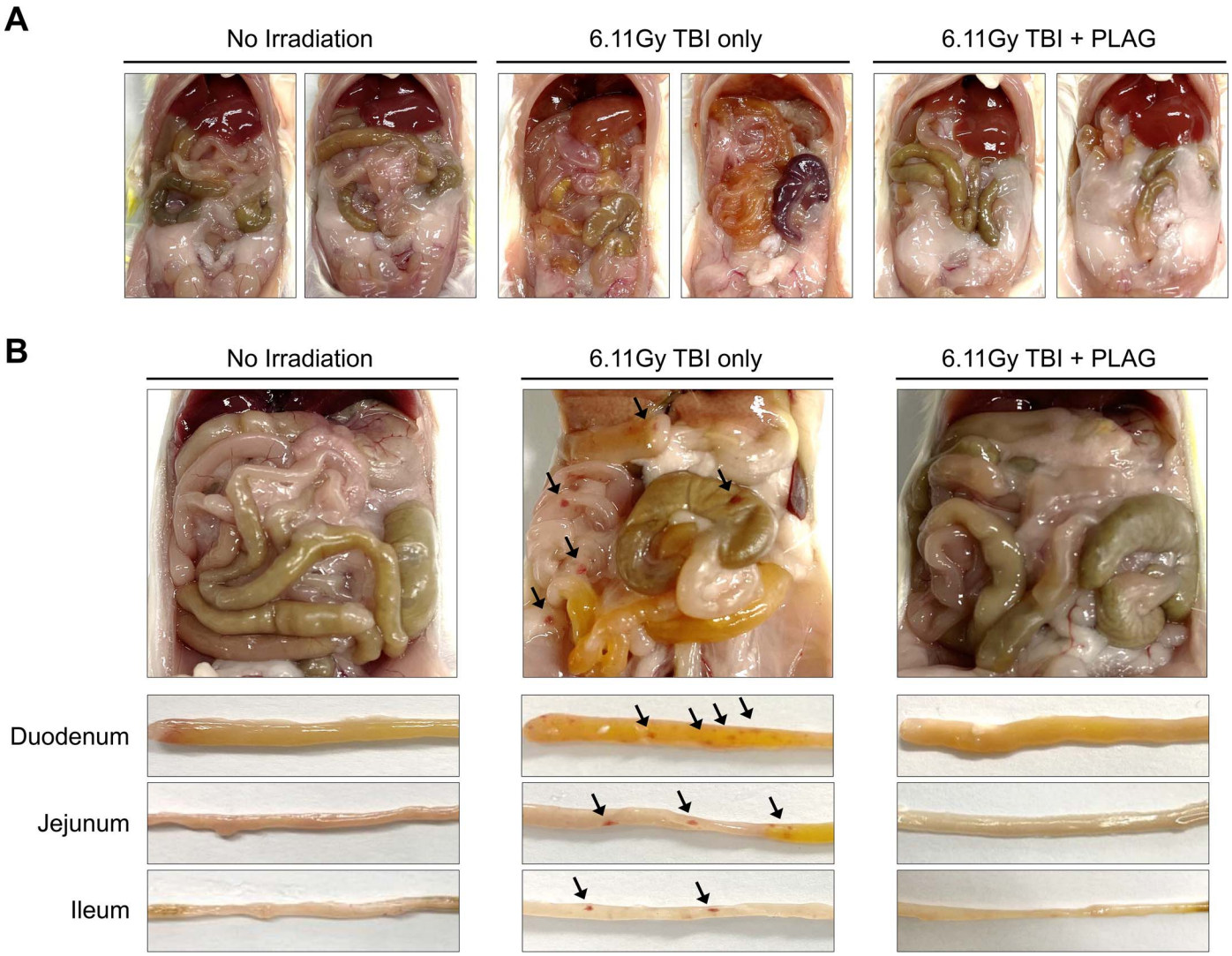

FIG. 1. Macroscopic view of gastrointestinal damage in irradiated mice. Panel A: Macroscopic observation was conducted on the GI tract after laparotomy of the BALB/c mice on day 15 after TBI. Panel B: An overview of the GI tract was conducted in all three parts of the small intestine, including the duodenum, jejunum, and ileum, from negative control, 6.11 Gy TBI only, and 6.11 Gy TBI + PLAG-treated mice. These results indicate that TBI induces multiple hemorrhagic spots (black arrows) in the GI tract and PLAG effectively mitigates the radiation-induced gastrointestinal injuries.

goblet cells markedly decreased on days 1, 3, 7, and 15 after TBI as compared to the non-irradiated group. In the PLAG-treated group, the number of goblet cells sharply decreased on days 1 and 3 after TBI; however, from day 7, the number almost recovered to the level observed in the non-irradiated group. This result indicates that PLAG promotes the population of mucin-producing goblet cells after the destruction of the intestinal epithelium by TBI.

PLAG Facilitates the Recovery of Crypt Cells by Promoting Cell Proliferation in the Intestinal Tissues Damaged after TBI

Since PLAG effectively facilitated the regeneration of the intestinal epithelium damaged by TBI, as shown in Figs. 2 and 3, we next investigated the effects of PLAG on the self-renewal potential of intestinal crypts after TBI. There is a population of undifferentiated intestinal stem cells at the crypt base that divides into progenitor or daughter cells for subsequent differentiation into the mature cell types necessary for normal gut function (*27*). To assess the proliferative capacity of intestinal stem cells, the levels of proliferating cell nuclear antigen (PCNA) in intestinal crypt cells were analyzed using immunohistochemistry. As shown in Fig. 4A and B, the number of PCNA-positive cells in the crypts was significantly reduced on day 1 after TBI and remained low until day 15 after TBI. However, in the PLAG-treated group, PCNA staining intensity and the number of PCNA-positive crypt cells were significantly increased on days 3, 7, and 15 after TBI as compared to the 6.11 Gy TBI-only group. These results confirm the tissue regenerative effects of PLAG on the GI tract damaged by TBI.

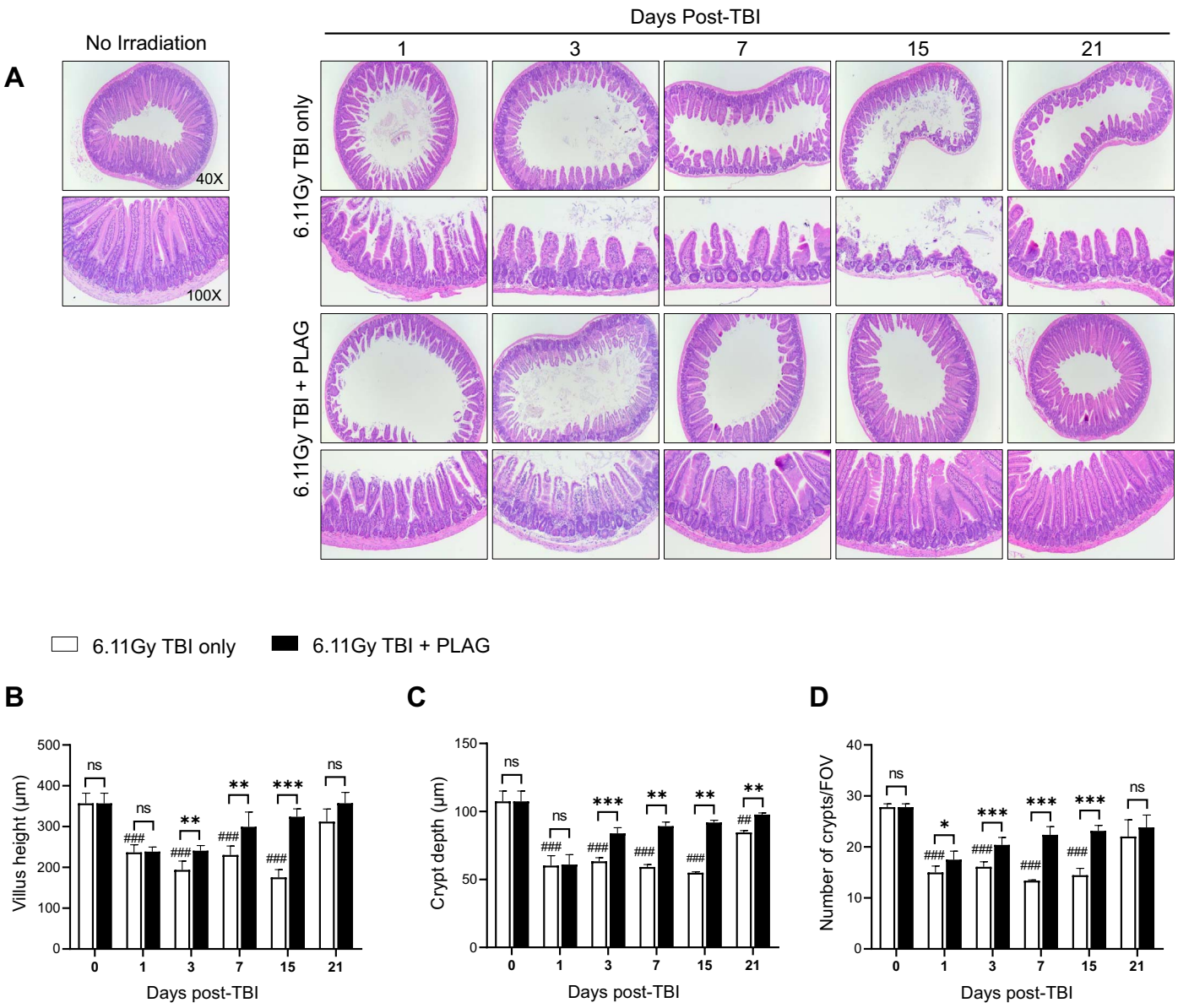

FIG. 2. PLAG facilitates the structural restoration of the intestinal tissues damaged by TBI. Panel A: Microscopic images of hematoxylin and eosin-stained jejunal intestinal tissues from the mice sacrificed at different time points (1, 3, 7, 15, and 21 days) after TBI. The images were captured at 40× and 100× magnification. The bar graph illustrates (panel B) villus height, (panel C) crypt depth, and (panel D) crypt numbers per field of view (FOV) based on intestinal histology. Data are expressed as bar graphs with mean ± standard deviation (SD) and analyzed with the Student t-test. #Negative control group vs. 6.11 Gy TBI only group; *6.11 Gy TBI only group vs. 6.11 Gy TBI + PLAG group. Statistical significance is denoted as follows: *ns*, not significant; #/*P < 0.05; ##/**P < 0.01; ###/***P < 0.001.

PLAG Restores Intestinal Functionality in TBI Mice

The primary function of the small intestine is to digest and absorb ingested nutrients as an energy source for the entire body (*28*). A D-xylose absorption assay is a widely used investigative tool to study the absorptive capacity of the small intestine in a variety of clinical and non-clinical settings. As it is a non-metabolizable sugar, D-xylose levels in the serum provide a reliable index of the functionality of the small intestine (*29*, *30*). We performed D-xylose absorption assays to determine the effects of radiation exposure and PLAG treatment on the absorptive function of the small intestine. Irradiation significantly impaired the intestinal absorption of D-xylose on days 7, 15, and 21 when compared to the non-irradiated group (day 0). PLAG significantly improved the intestinal absorptive capacity of TBI mice from day 15 onwards, reaching that of the non-irradiated group (Fig. 5). These findings suggest that PLAG promotes the reconstitution of the intestinal epithelium, resulting in the restoration of intestinal functionality after TBI.

PLAG Reduces Intestinal Injury-induced Bacterial Translocation in TBI Mice

Many studies demonstrated that the high mortality rates of mice exposed to a lethal dose of gamma ray are associated with gut bacteria-related infectious complications

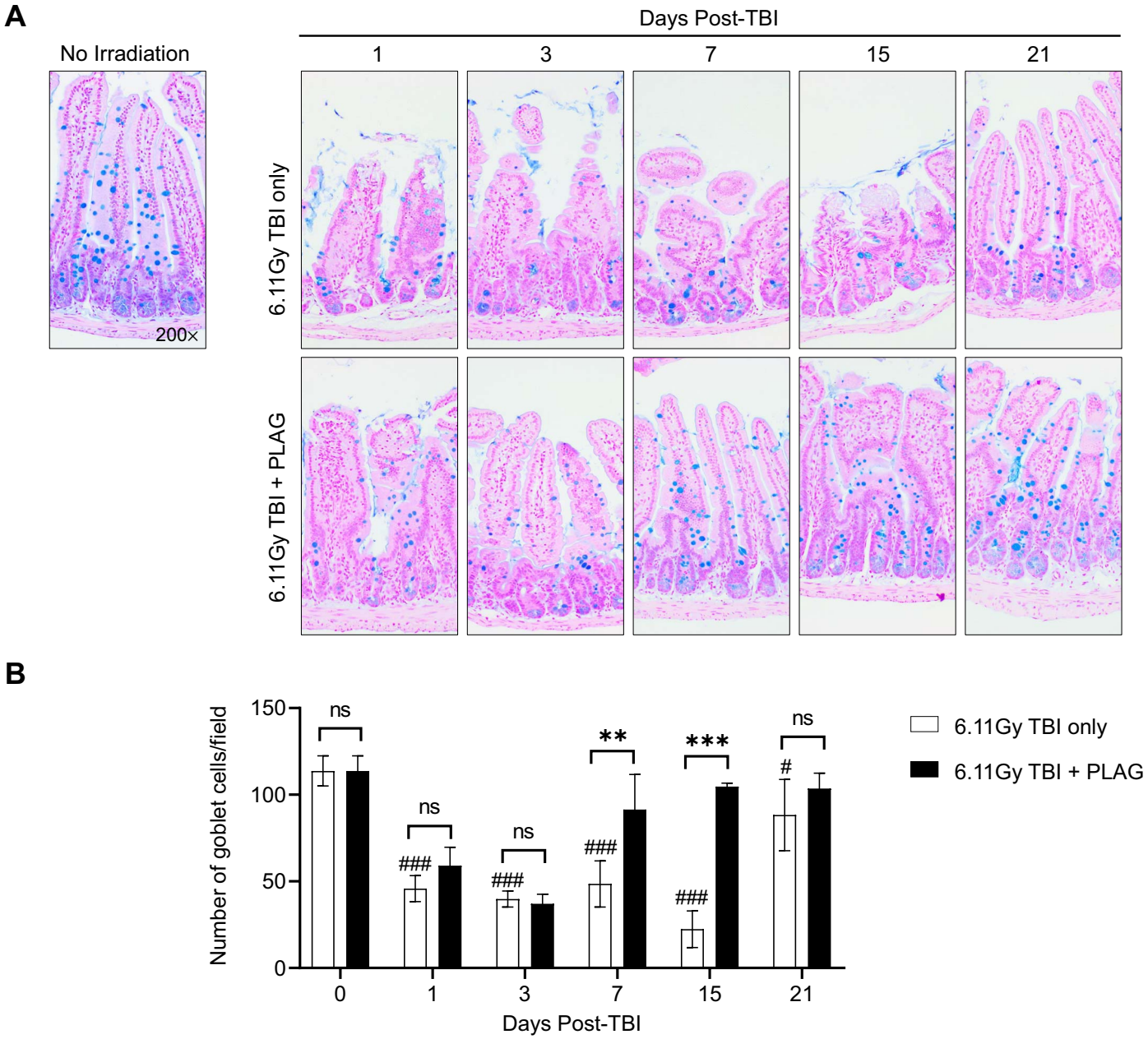

FIG. 3. PLAG increases mucin secretion by promoting the recovery of goblet cells in the intestinal tissues damaged by TBI. Panel A: Microscopic images of Alcian blue (AB) and eosin-stained jejunal intestinal tissues from the mice sacrificed at different time points (1, 3, 7, 15, and 21 days) after TBI. The images were captured at 200× magnification. The blue spots indicate AB-stained mucin produced by goblet cells. Panel B: The number of goblet cells per field was measured for quantitative analysis. Data are expressed as bar graphs with mean ± SD and analyzed with the Student t-test. #Negative control group vs. 6.11 Gy TBI only group; *6.11 Gy TBI only group vs. 6.11 Gy TBI + PLAG group. Statistical significance is denoted as follows: *ns*, not significant; #/*P < 0.05; ##/**P < 0.01; ###/***P < 0.001.

(*23*, *24*, *31*). Since PLAG was previously demonstrated to restore radiation-induced intestinal damage, we next investigated the effects of PLAG on intestinal injury-induced gut bacterial translocation in TBI mice. The experimental design for intestinal injury-induced bacterial translocation in TBI mice is shown in Fig. 6A. First, we investigated the role of infectious complications in the mortality of our 6.11 Gy ($LD_{70/30}$) TBI mouse model by decontaminating the mice with an antibiotic mixture in drinking water. As a result, 40% of the mice were found dead within 11 days after irradiation in the 6.11 Gy TBI-only group, whereas the mice decontaminated with the antibiotic mixture all survived (Fig. 6B). However, 90% of decontaminated and irradiated mice died after *E. faecalis* oral infection, supporting the idea that high mortality after TBI is closely associated with gut bacteria-related infectious complications. Conversely, administration of PLAG (250 mg/kg) significantly enhanced survival to 70% (Fig. 6B). To examine the translocation of *E. faecalis* to other organs, a colony formation assay was performed

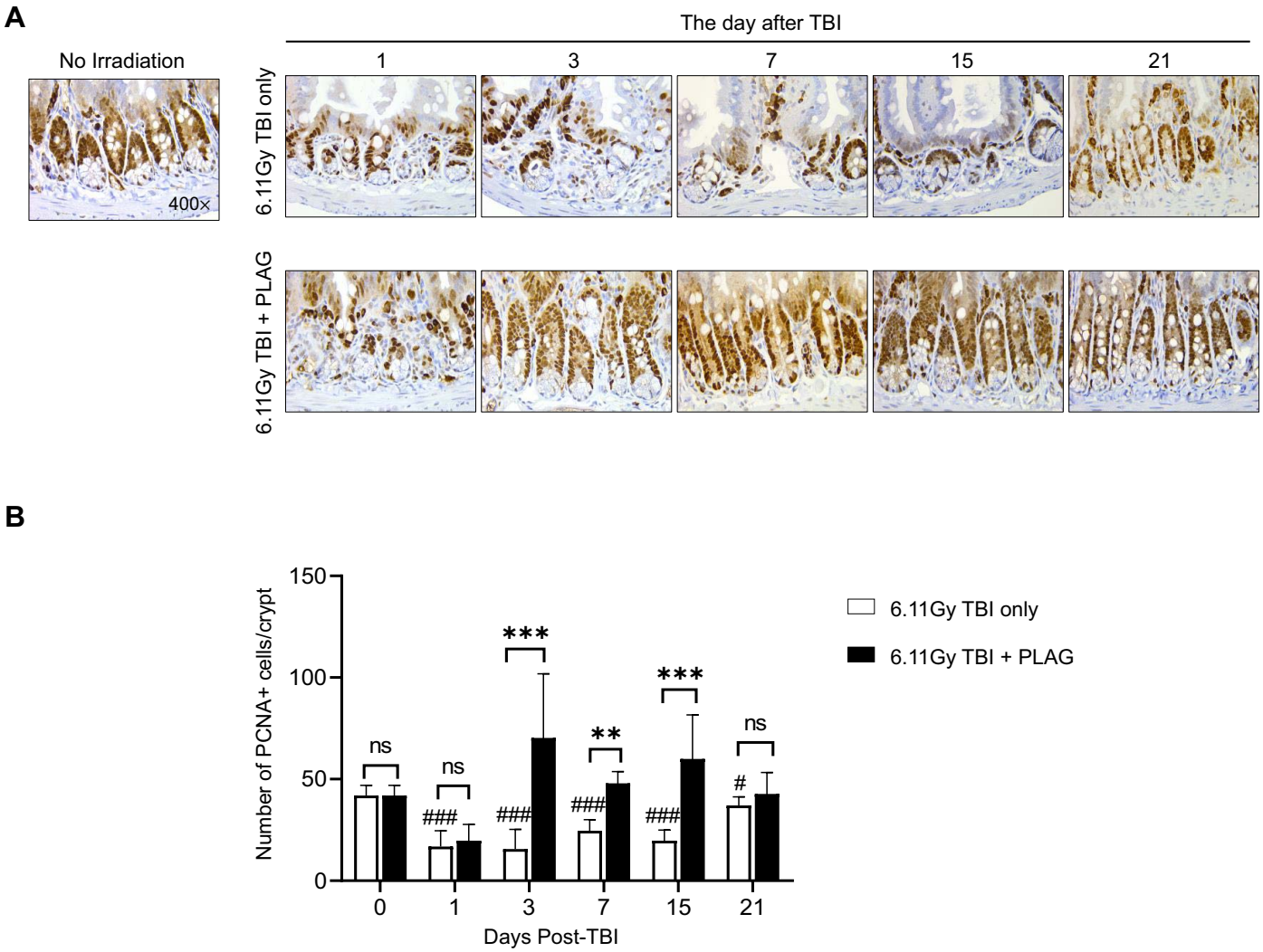

FIG. 4. PLAG facilitates the recovery of crypt cells by promoting cell proliferation in the intestinal tissues damaged by TBI. Panel A: Immunohistochemistry of the jejunal tissue sections at days 1, 3, 7, and 21 stained with a specific PCNA Ab and counterstained with hematoxylin. The images were captured at 400× magnification. Panel B: The number of PCNA-positive cells per crypt in the jejunal tissues was measured for quantitative analysis. PLAG effectively increased the number of PCNA-positive cells in the intestinal crypts. Data are expressed as bar graphs with mean ± SD and analyzed with the Student t-test. #Negative control group vs. 6.11 Gy TBI only group; *6.11 Gy TBI only group vs. 6.11 Gy TBI + PLAG group. Statistical significance is denoted as follows: ns, not significant; #/*P < 0.05; ##/**P < 0.01; ###/***P < 0.001.

using blood, as well as lung and liver homogenates. As shown in Fig. 6C, more than 70% of the organs were found to be *E. faecalis* positive on days 1, 3, 5, and 7 after oral infection, whereas PLAG substantially decreased the percentage of organs positive for *E. faecalis*. Furthermore, *E. faecalis*-positive organs in the PLAG-treated group showed significantly lower growth rates than their counterparts (Fig. 6D). Taken together, these results indicate that PLAG not only promotes the regeneration of injured intestinal epithelium but also prevents infectious complications caused by gut bacterial translocation after TBI.

PLAG Reduces HMGB1 Release from the Intestinal Crypt Cells Damaged by TBI

Cells damaged or dying in response to radiation exposure can alert the immune system to dangerous conditions by releasing DAMPs (*18*). A previous study demonstrated that PLAG ameliorated neutrophilic inflammation in tongue tissues by reducing both serum and cytoplasmic levels of high-motility group box *1* (HMGB1), a typical endogenous DAMP, in a murine model of chemotherapy and radiation-induced oral mucositis (*25*). Thus, we assessed the effects of PLAG on the release of HMGB1 in both intestinal crypt cells and the serum of TBI mice. As shown in Fig. 7A, cytoplasmic HMGB1 was intensively stained in the intestinal crypt cells of the 6.11 Gy TBI-only group on days 7, 15, and 21 after TBI, indicating that HMGB1 originally located in the nucleus was translocated to the cytoplasm in these mice. In contrast, HMGB1 remained in the nucleus of the PLAG-treated group. Next, we examined the serum levels of HMGB1 on day 15 after TBI by Western blotting (Fig. 7B). The relative band intensities obtained from

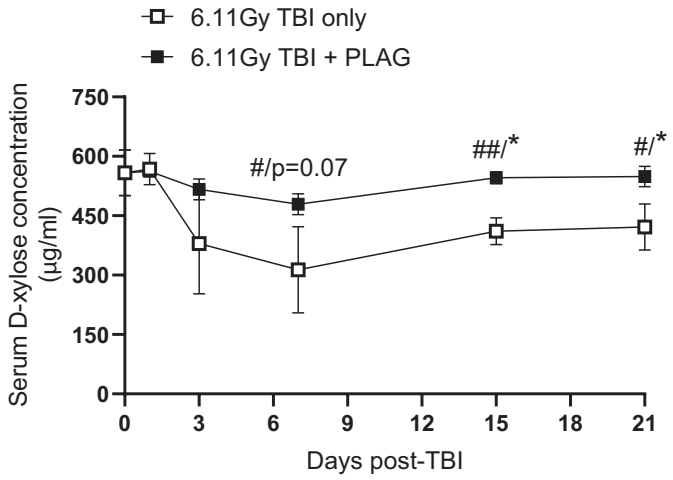

FIG. 5. PLAG restores intestinal functionality in TBI mice. Effects of PLAG on intestinal functional regeneration in TBI mice by D-xylose absorption assay. Serum D-xylose concentration (μg/ml) was measured on days 1, 3, 7, 15, and 21 after TBI. Data are expressed as bar graphs with mean ± SD and analyzed the Student *t*-test. #Negative control group vs. 6.11 Gy TBI only group; *6.11 Gy TBI only group vs. 6.11 Gy TBI + PLAG group. Statistical significance is denoted as follows: #/*$P < 0.05$; ##/*$P < 0.01$.

the band image in Fig. 7B showed that PLAG significantly reduced the serum levels of HMGB1 in TBI mice (Fig. 7C).

PLAG Regulates the Necroptosis Signaling Pathway in Radiation-Damaged Intestinal Crypt Cells

To assess whether the release of HMGB1 was associated with necroptotic damage in intestinal crypt cells, the phosphorylated form of MLKL and a marker of necroptosis activation, was examined by immunohistochemistry (Fig. 8A). DAB staining intensities were quantified and compared between groups using Student's t-test (Fig. 8B). The results showed that the level of MLKL phosphorylation was significantly elevated in the intestinal crypt cells of the 6.11 Gy TBI-only group on days 3, 7, 15, and 21 after TBI, whereas administration of PLAG significantly reduced MLKL phosphorylation in radiation-damaged intestinal crypt cells. These results indicate that PLAG effectively regulates the necroptosis signaling pathway and the release of HMGB1 in radiation-damaged intestinal crypts.

DISCUSSION

The gastrointestinal system is one of the most radiosensitive organ systems in the body owing to its deleterious effects of radiation, especially on cells undergoing mitosis. The cells that make up the lining of the intestinal epithelium are replaced with newly differentiated cells every 3–5 days as clonogenic crypt cells continue to migrate upward as they differentiate into nutrient-absorbing enterocytes, mucus-secreting goblet cells, and hormone-secreting enteroendocrine cells. Radiation-induced death of clonogenic crypt cells, particularly intestinal stem cells, impairs intestinal homeostasis by demolishing the mucosal barrier, which physically and biochemically segregates host tissue and gut-inhabiting bacteria. Therefore, radiation countermeasures to treat GI-ARS should be developed to determine whether candidates can prevent radiation-induced damage to clonogenic crypt cells or facilitate the regeneration of the intestinal epithelium that was already disintegrated by radiation exposure. In this study, we investigated the potential of the PLAG as a radiation countermeasure against GI-ARS. Our results showed that PLAG promotes the regeneration and repopulation of the intestinal epithelium by stimulating the proliferation of crypt cells, resulting in improved nutrient absorption by enterocytes and protection from gut bacterial invasion by rebuilding the mucosal barrier. Moreover, the inhibition of necroptosis signaling and the reduction of HMGB1 release by PLAG contributed to the mitigation of radiation-induced GI injury. The mitigation of H-ARS by PLAG, as reported previously (*20*, *21*), and that of GI-ARS demonstrated here make this drug a promising candidate as a radiation countermeasure against radiation injury caused by severe life-threatening radiation exposure.

In this study, we demonstrated that PLAG rapidly restored intestinal epithelium collapse caused by radiation exposure by promoting cell proliferation within the crypts. This finding was consistent with our previous results, which showed that PLAG accelerated bone marrow recovery after TBI in mice. Crypt base columnar (CBC) cells, which express leucine-rich repeat-containing G protein-coupled receptor 5 (Lgr5), are rapidly cycling and self-renewing intestinal stem cells that are responsible for maintaining intestinal homeostasis in the steady state but are highly susceptible to exogenous damage such as chemicals, pathogens, or irradiation (*32*). Another stem cell pool replaced the Lgr5+ CBC cells when the intestinal epithelium was injured. These types of intestinal stem cells are quiescent in the normal state but become active and act as a major cell supply for epithelial regeneration after the loss of Lgr5+ CBC cells. Quiescent intestinal stem cells are marked by unique markers such as Bmi1, Tert, Hopx, Krt19, Clu, Mex3a, and Lrig1 (*32–35*). We have demonstrated the efficacy of PLAG on the regeneration of the hematopoietic system, which was injured by radiation or anticancer drugs in previous studies (*20–22*), and we confirmed that the efficacy of PLAG works identically in the gastrointestinal system in the current study. When all these studies are combined, it is reasonable to assume that PLAG has some stimulatory effects on quiescent stem cells or their niche after radiation damage. Therefore, further studies to decipher the cellular targets and molecular mechanisms of PLAG are required to better understand the physiological and molecular roles of PLAG in ARS.

Damage to the GI tract from radiation or accidental radiation exposure is usually accompanied by damage to other organs. TBI doses that induce GI-ARS usually deplete bone marrow cells, leading to the manifestation of H-ARS (*36*). Therefore, GI-ARS is closely linked to the

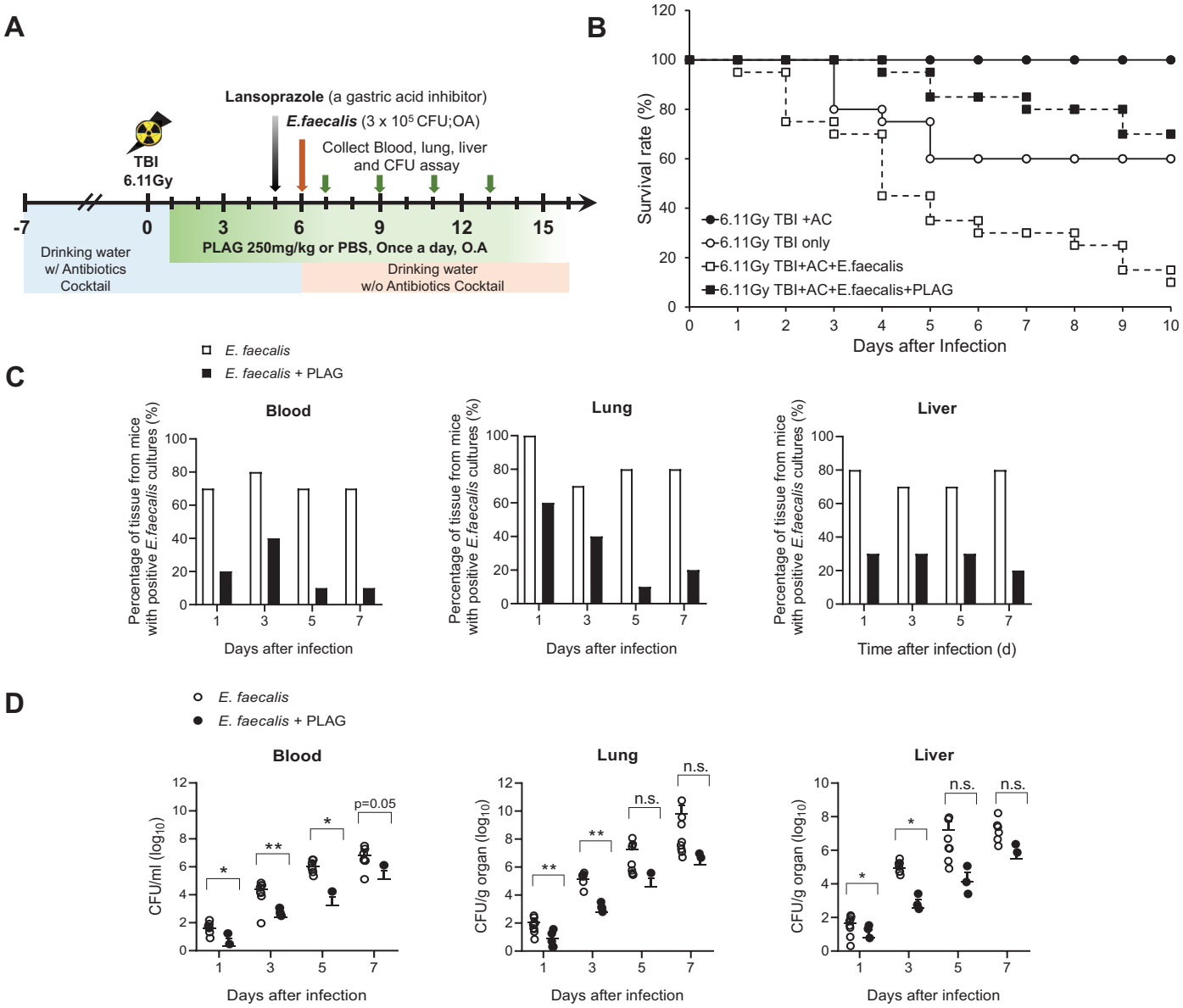

FIG. 6. PLAG reduces intestinal injury-induced bacterial translocation in TBI mice. Panel A: Schematic diagram of intestinal injury-induced spontaneous bacterial translocation in TBI mice. The experimental procedures are described in Materials and Methods in detail. Panel B: Survival was monitored for 15 days starting from *E. faecalis* oral infection. P = 0.0018, 6.11 Gy TBI + antibiotics cocktail (AC) vs. 6.11 Gy TBI only; P < 0.001, 6.11 Gy TBI + AC + *E. faecalis* vs. 6.11 Gy TBI + AC + *E. faecalis* + PLAG (log-rank test). PLAG reduces (panel C) occurrence rate with positive *E. faecalis* cultures and (panel D) bacterial growth in blood, lung, and liver tissues of TBI mice orally infected with *E. faecalis*. Data are expressed as bar graphs with mean ± SD and analyzed with the Student t-test. Statistical significance is denoted as follows: *P < 0.05; **P < 0.01; ***P < 0.001.

hematopoietic system in that the extent of bone marrow damage can determine the host's immunity against infectious complications due to gut microbiota translocation through the impaired intestinal mucosal barrier (*15*). It has been reported that the mortality rates from GI-ARS differ depending on the implementation and extent of bone marrow sparing in some experimental settings (*37*, *38*). Thus, it is reasonable to assume that the effects of PLAG on GI-ARS, including the structural and functional recovery of intestinal epithelium and the mitigation of gut bacterial translocation-associated mortality and morbidity, are partly attributed to its mitigating effects on H-ARS. We previously verified that administration of PLAG improves peripheral blood cell recovery by accelerating bone marrow cellularity in TBI mice (*20*, *21*).

Gut bacterial translocation through an impaired mucosal barrier is a major life-threatening factor in GI-ARS. The translocation of indigenous gut bacteria through the injured gut mucosa can lead to invasion into neighboring or distant organs that are normally sterile, subsequently resulting in systemic inflammatory response syndrome (SIRS) or septic death, especially in conjunction with an immunocompromised status (*39*). Moreover, high levels of cytokines and chemokines, such as TNF,

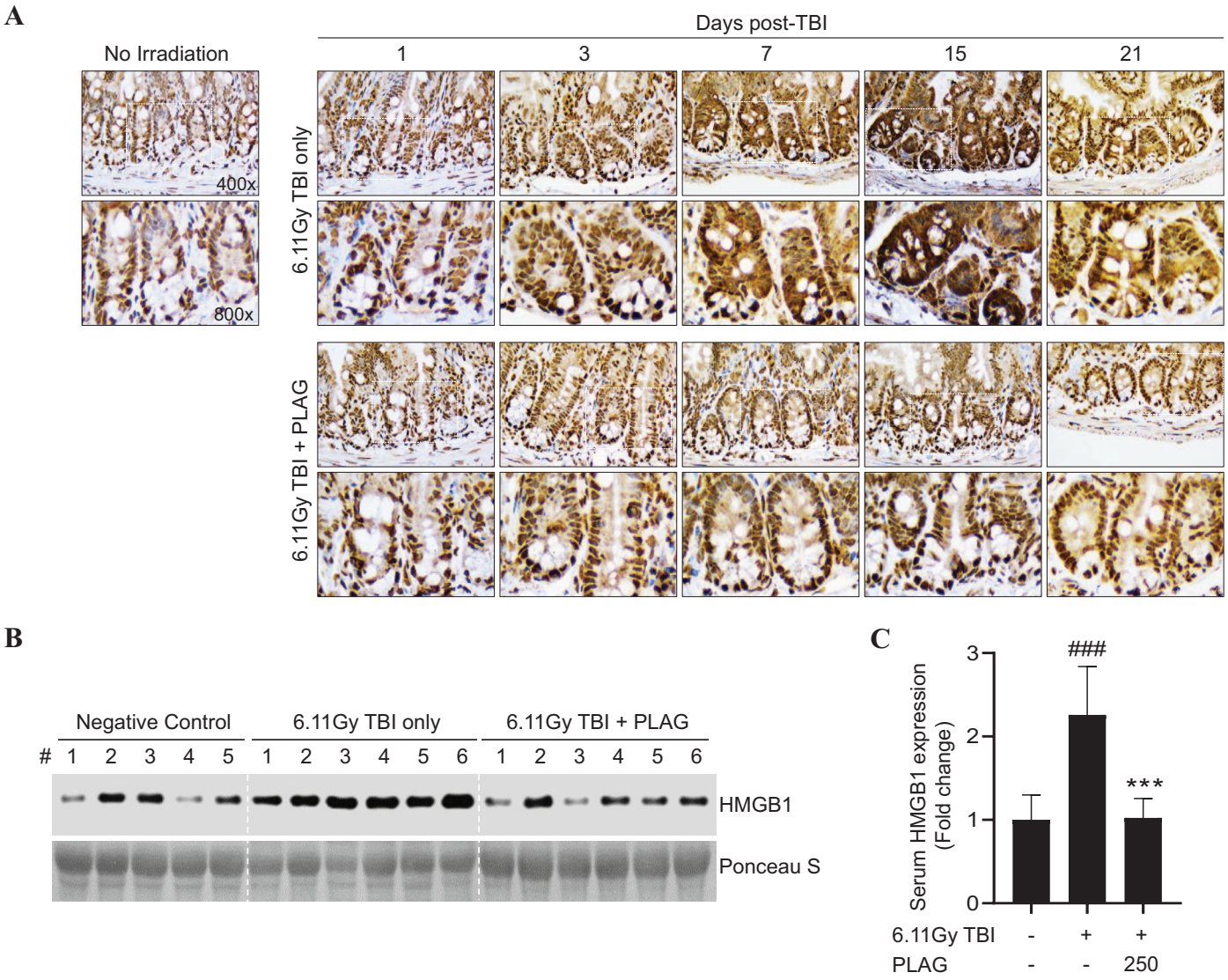

FIG. 7. PLAG reduces HMGB1 release from TBI-damaged intestinal crypt cells. Panel A: Immunohistochemistry of small intestine sections at 0, 1, 3, 7, 15, and 21 days after TBI stained with a specific HMGB1 Ab and counterstained with hematoxylin. The images were captured at 400× and 800× magnification. Panel B: The protein level of HMGB1 in the blood was detected by Western blotting. Panel C: The band densities of HMGB1 were quantified using ImageJ software. Data are expressed as bar graphs with mean ± SD and analyzed with one-way ANOVA with a Turkey post-test. #Negative control group vs. 6.11 Gy TBI only group; *6.11 Gy TBI only group vs. 6.11 Gy TBI + PLAG group. Statistical significance is denoted as follows: ###/***$P < 0.001$.

IL-1β, IL-6, IL-8, CXCL1, and CXCL2, produced by the infected tissue macrophages and adjacent endothelial cells through the activation of pattern recognition receptors (PRR) can cause serious tissue damage and loss of function (*40*). Previously, PLAG was shown to effectively attenuate pro-inflammatory cytokines/chemokines, including IL-6, CXCL1, and CXCL2, which are produced by TBI between 13 and 21 days after TBI (*20*). In this study, we concluded that the reduction of cytokines/chemokines by PLAG was correlated with an improvement in peripheral blood cell recovery and survival rate (*20*). In addition, we demonstrated that PLAG effectively prevented gut bacterial translocation through a radiation-damaged mucosal barrier in the current study. We presume that the explosive increase in inflammatory cytokines between 13 and 21 days after TBI identified in previous study results from gut bacterial translocation through increased mucosal barrier permeability and immunodeficiency after radiation exposure (*20*). In addition, we believe that the prevention of gut bacterial translocation by PLAG partially contributed to the downregulation of the cytokine surge observed between 13 and 21 days after TBI and the subsequent mortality.

Necroptosis is a type of programmed cell death that mimics apoptosis and necrosis (*41*). Radiation induces the activation of the necroptosis signaling pathway, and dysregulation of necroptosis is associated with many pathological conditions, including cancer, bacterial infection, viral infection,

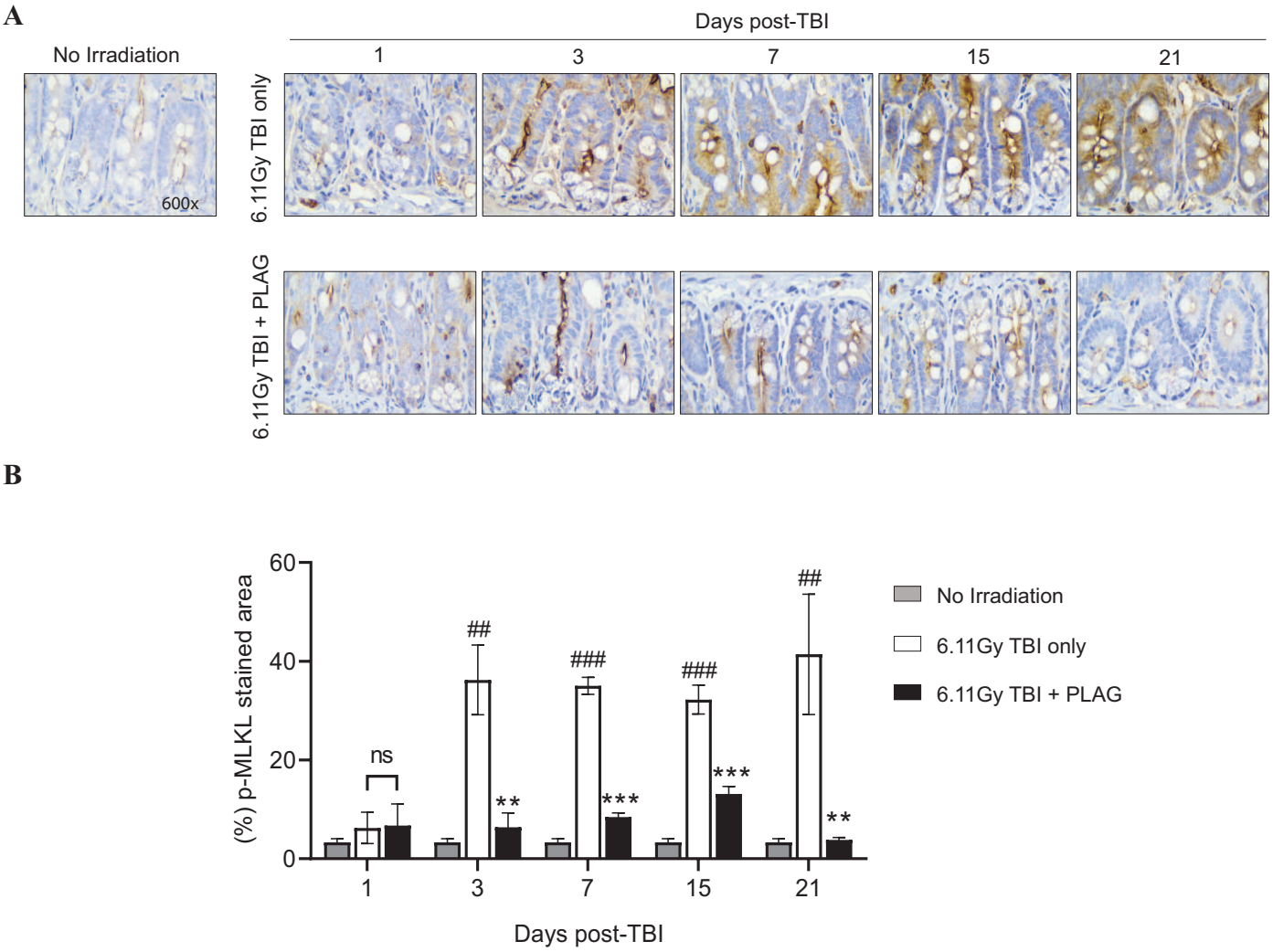

FIG. 8. PLAG regulates the necroptosis signaling pathway in TBI-damaged intestinal crypt cells. Panel A: Immunohistochemistry of small intestine sections at 0, 1, 3, 7, 15, and 21 days after TBI stained with a specific phosphor-MLKL Ab and counterstained with hematoxylin. The images were captured at 600× magnification. Panel B: Quantification of phosphor-MLKL staining intensity in the intestinal crypt cells. Data are expressed as bar graphs with mean ± SD and analyzed with the Student t-test. #Negative control group vs. 6.11 Gy TBI only group; *6.11 Gy TBI only group vs. 6.11 Gy TBI + PLAG group. Statistical significance is denoted as follows: ns, not significant; #/*P < 0.05; ##/**P < 0.01; ###/***P < 0.001.

and neurodegenerative diseases (*18*, *41–45*). In this study, we demonstrated that necroptosis is a key mechanism underlying TBI-induced GI damage and demonstrated the inhibitory effects of PLAG on radiation-induced necroptosis activation, as evidenced by reduced HMGB1 release and MLKL phosphorylation in intestinal crypt cells. Since GI-ARS is a pathological GI tract condition with complex and multifactorial mechanisms that are difficult to fully understand, necroptosis is not the only cell death mode that intensifies the symptoms of GI-ARS. Therefore, it is worthwhile studying the effects of PLAG on other modes of cell death in the context of radiation injury.

ACKNOWLEDGMENTS

PLAG has been approved for Orphan Drug Designation by the US Food and Drug Administration (FDA) for the treatment of acute radiation syndrome under the name of EC-18. All authors are employees of Enzychem Life Sciences. The corresponding author, Jae Wha Kim, declares that the research was conducted in the absence of any commercial or financial relationships that could be constructed as a potential conflict of interest. The author, Ki-young Sohn, is a president of Enzychem Lifesciences. The remaining authors are employees of Enzychem Lifesciences.

Received: April 30, 2024; accepted: July 23, 2024; published online: August 27, 2024

REFERENCES

1. Ryu SH, Park JH, Jeong ES, Choi SY, Ham SH, Park JI, et al. Establishment of a mouse model of 70% lethal dose by total-body irradiation. Lab Anim Res 2016; 32, 116-21.
2. Singh VK, Seed TM, Acute radiation syndrome drug discovery using organ-on-chip platforms. Expert Opin Drug Discov 2022; 17, 865-78.
3. Singh VK, Seed TM, Development of gamma-tocotrienol as a radiation medical countermeasure for the acute radiation syndrome: current

status and future perspectives. Expert Opin Investig Drugs 2023; 32, 25-35.

4. Singh VK, Seed TM, Radiation countermeasures for hematopoietic acute radiation syndrome: growth factors, cytokines and beyond. Int J Radiat Biol 2021; 97, 1526-47.

5. Singh VK, Newman VL, Berg AN, MacVittie TJ, Animal models for acute radiation syndrome drug discovery. Expert Opin Drug Discov 2015; 10, 497-517.

6. Hollingsworth BA, Cassatt DR, DiCarlo AL, Rios CI, Satyamitra MM, Winters TA, et al. Acute Radiation Syndrome and the Microbiome: Impact and Review. Front Pharmacol 2021; 12, 643283.

7. Potten CS, A comprehensive study of the radiobiological response of the murine (BDF1) small intestine. Int J Radiat Biol 1990; 58, 925-73.

8. Singh VK, Seed TM, A review of radiation countermeasures focusing on injury-specific medicinals and regulatory approval status: part I. Radiation sub-syndromes, animal models and FDA-approved countermeasures. Int J Radiat Biol 2017; 93, 851-69.

9. Arike L, Seiman A, van der Post S, Rodriguez Pineiro AM, Ermund A, et al. Protein Turnover in Epithelial Cells and Mucus along the Gastrointestinal Tract Is Coordinated by the Spatial Location and Microbiota. Cell Rep 2020; 30, 1077-87 e3.

10. Elliott TB, Deutz NE, Gulani J, Koch A, Olsen CH, Christensen C, et al. Gastrointestinal acute radiation syndrome in Gottingen minipigs (Sus scrofa domestica). Comp Med 2014; 64, 456-63.

11. Venkateswaran K, Shrivastava A, Agrawala PK, Prasad AK, Devi SC, Manda K, et al. Mitigation of radiation-induced gastrointestinal injury by the polyphenolic acetate 7, 8-diacetoxy-4-methylthiocoumarin in mice. Sci Rep 2019; 9, 14134.

12. Farese AM, Bennett AW, Gibbs AM, Hankey KG, Prado K, Jackson W, 3rd, et al. Efficacy of Neulasta or Neupogen on H-ARS and GI-ARS Mortality and Hematopoietic Recovery in Nonhuman Primates After 10-Gy Irradiation With 2.5% Bone Marrow Sparing. Health Phys 2019; 116, 339-53.

13. MacVittie TJ, Bennett AW, Farese AM, Taylor-Howell C, Smith CP, Gibbs AM, et al. The Effect of Radiation Dose and Variation in Neupogen(R) Initiation Schedule on the Mitigation of Myelosuppression during the Concomitant GI-ARS and H-ARS in a Nonhuman Primate Model of High-dose Exposure with Marrow Sparing. Health Phys 2015; 109, 427-39.

14. Kenchegowda D, Bolduc DL, Kurada L, Blakely WF, Severity scoring systems for radiation-induced GI injury - prioritization for use of GI-ARS medical countermeasures. Int J Radiat Biol 2023; 99, 1037-45.

15. Booth C, Tudor G, Tudor J, Katz BP, MacVittie TJ, Acute gastrointestinal syndrome in high-dose irradiated mice. Health Phys 2012; 103, 383-99.

16. Lewanski CR, Gullick WJ, Radiotherapy and cellular signalling. Lancet Oncol 2001; 2, 366-70.

17. Fukumoto R, Cary LH, Gorbunov NV, Lombardini ED, Elliott TB, Kiang JG, Ciprofloxacin modulates cytokine/chemokine profile in serum, improves bone marrow repopulation, and limits apoptosis and autophagy in ileum after whole body ionizing irradiation combined with skin-wound trauma. PLoS One 2013; 8, e58389.

18. Yamaga S, Aziz M, Murao A, Brenner M, Wang P, DAMPs and radiation injury. Front Immunol 2024; 15, 1353990.

19. Huang Z, Epperly M, Watkins SC, Greenberger JS, Kagan VE, Bayir H, Necrostatin-1 rescues mice from lethal irradiation. Biochim Biophys Acta 2016; 1862, 850-56.

20. Kim YJ, Jeong J, Park K, Sohn KY, Yoon SY, Kim JW, Mitigation of Hematopoietic Syndrome of Acute Radiation Syndrome by 1-Palmitoyl-2-linoleoyl-3-acetyl-rac-glycerol (PLAG) is Associated with Regulation of Systemic Inflammation in a Murine Model of Total-Body Irradiation. Radiat Res 2021; 196, 55-65.

21. Kim YJ, Jeong J, Shin SH, Lee DY, Sohn KY, Yoon SY, et al. Mitigating Effects of 1-Palmitoyl-2-linoleoyl-3-acetyl-rac-glycerol (PLAG) on Hematopoietic Acute Radiation Syndrome after Total-Body Ionizing Irradiation in Mice. Radiat Res 2019; 192, 602-11.

22. Jeong J, Kim YJ, Lee DY, Sohn KY, Yoon SY, Kim JW, Mitigating Effect of 1-Palmitoyl-2-Linoleoyl-3-Acetyl-Rac-Glycerol (PLAG) on a Murine Model of 5-Fluorouracil-Induced Hematological Toxicity. Cancers (Basel) 2019; 11.

23. Suzuki F, Loucas BD, Ito I, Asai A, Suzuki S, Kobayashi M, Survival of Mice with Gastrointestinal Acute Radiation Syndrome through Control of Bacterial Translocation. J Immunol 2018; 201, 77-86.

24. Kobayashi M, Nakamura K, Cornforth M, Suzuki F, Role of M2b macrophages in the acceleration of bacterial translocation and subsequent sepsis in mice exposed to whole body [137Cs] gamma-irradiation. J Immunol 2012; 189, 296-303.

25. Choi S, Shin SH, Lee HR, Sohn KY, Yoon SY, Kim JW, 1-Palmitoyl-2-linoleoyl-3-acetyl-rac-glycerol ameliorates chemoradiation-induced oral mucositis. Oral Dis 2020; 26, 111-21.

26. Herath M, Hosie S, Bornstein JC, Franks AE, Hill-Yardin EL, The Role of the Gastrointestinal Mucus System in Intestinal Homeostasis: Implications for Neurological Disorders. Front Cell Infect Microbiol 2020; 10, 248.

27. Umar S, Intestinal stem cells. Curr Gastroenterol Rep 2010; 12, 340-8.

28. Cheng LK, O'Grady G, Du P, Egbuji JU, Windsor JA, Pullan AJ, Gastrointestinal system. Wiley Interdiscip Rev Syst Biol Med 2010; 2, 65-79.

29. Craig RM, Atkinson AJ, Jr., D-xylose testing: a review. Gastroenterology 1988; 95, 223-31.

30. Fordtran JS, Soergel KH, Ingelfinger FJ, Intestinal absorption of D-xylose in man. N Engl J Med 1962; 267, 274-9.

31. Ito I, Loucas BD, Suzuki S, Kobayashi M, Suzuki F, Glycyrrhizin Protects gamma-Irradiated Mice from Gut Bacteria-Associated Infectious Complications by Improving miR-222-Associated Gas5 RNA Reduction in Macrophages of the Bacterial Translocation Site. J Immunol 2020; 204, 1255-62.

32. Kurokawa K, Hayakawa Y, Koike K, Plasticity of Intestinal Epithelium: Stem Cell Niches and Regulatory Signals. Int J Mol Sci 2020; 22.

33. Asfaha S, Hayakawa Y, Muley A, Stokes S, Graham TA, Ericksen RE, et al. Krt19(+)/Lgr5(-) Cells Are Radioresistant Cancer-Initiating Stem Cells in the Colon and Intestine. Cell Stem Cell 2015; 16, 627-38.

34. Montgomery RK, Carlone DL, Richmond CA, Farilla L, Kranendonk ME, Henderson DE, et al. Mouse telomerase reverse transcriptase (mTert) expression marks slowly cycling intestinal stem cells. Proc Natl Acad Sci U S A 2011; 108, 179-84.

35. Tian H, Biehs B, Warming S, Leong KG, Rangell L, Klein OD, et al. A reserve stem cell population in small intestine renders Lgr5-positive cells dispensable. Nature 2011; 478, 255-9.

36. MacVittie TJ, Bennett A, Booth C, Garofalo M, Tudor G, Ward A, et al. The prolonged gastrointestinal syndrome in rhesus macaques: the relationship between gastrointestinal, hematopoietic, and delayed multi-organ sequelae after acute, potentially lethal, partial-body irradiation. Health Phys 2012; 103, 427-53.

37. Huang W, Yu J, Liu T, Tudor G, Defnet AE, Zalesak S, et al. Proteomic Evaluation of the Natural History of the Acute Radiation Syndrome of the Gastrointestinal Tract in a Non-human Primate Model of Partial-body Irradiation with Minimal Bone Marrow Sparing Includes Dysregulation of the Retinoid Pathway. Health Phys 2020; 119, 604-20.

38. Kumar P, Wang P, Tudor G, Booth C, Farese AM, MacVittie TJ, et al. Evaluation of Plasma Biomarker Utility for the Gastrointestinal Acute Radiation Syndrome in Non-human Primates after

Partial Body Irradiation with Minimal Bone Marrow Sparing through Correlation with Tissue and Histological Analyses. Health Phys 2020; 119, 594-603.

39. Vaishnavi C, Translocation of gut flora and its role in sepsis. Indian J Med Microbiol 2013; 31, 334-42.

40. Chousterman BG, Swirski FK, Weber GF, Cytokine storm and sepsis disease pathogenesis. Semin Immunopathol 2017; 39, 517-28.

41. Dhuriya YK, Sharma D, Necroptosis: a regulated inflammatory mode of cell death. J Neuroinflammation 2018; 15, 199.

42. Robinson N, McComb S, Mulligan R, Dudani R, Krishnan L, Sad S, Type I interferon induces necroptosis in macrophages during infection with Salmonella enterica serovar Typhimurium. Nat Immunol 2012; 13, 954-62.

43. Roca FJ, Ramakrishnan L, TNF dually mediates resistance and susceptibility to mycobacteria via mitochondrial reactive oxygen species. Cell 2013; 153, 521-34.

44. Nogusa S, Thapa RJ, Dillon CP, Liedmann S, Oguin TH, 3rd, Ingram JP, et al. RIPK3 Activates Parallel Pathways of MLKL-Driven Necroptosis and FADD-Mediated Apoptosis to Protect against Influenza A Virus. Cell Host Microbe 2016; 20, 13-24.

45. Wu JR, Wang J, Zhou SK, Yang L, Yin JL, Cao JP, et al. Necrostatin-1 protection of dopaminergic neurons. Neural Regen Res 2015; 10, 1120-4.